

Studies of Pulsed Signals in High-precision Experiments (Antarctica)

Sergey N. Shapovalov*, Oleg A. Troshichev†, Vacheslav I. Povazhny‡ and Igor V. Moskvin**

SSC Arctic and Antarctic Research Institute. 38 Beringa st., 199397 St-Petersburg, Russia

*E-mail: shapovalov@aari.ru; †E-mail: olegtro@aari.ru; ‡E-mail: povazviach@gmail.com; **E-mail: im-geo@aari.ru

The paper presents the results of studies on pulsed signals in photocurrent (PCC-2 instrument), in the 565-nm LED spectrum, and in the atmospheric zenith spectrum (342.5 nm). According to the results of statistical analysis of data measurements for the period from 24.04.04 till 01.02.06 a correlation between the temporal distribution of pulsed signals in photocurrent PCC-2 and CA F10.7 cm (2800 MHz) index and the total solar radiation (TSI) was established. In the course of the parallel measurements of photocurrent in PCC-2 and fluctuations in the spectra frequencies of the LED and the atmosphere zenith, based on the average daily values of the standard deviation, the identical trend in the photocurrent pulse signals (PCC-2) and the fluctuations at 520-nm LED spectrum and 342.5-nm atmosphere zenith spectrum was detected (AvaSpec-2048 spectrometer).

1 Introduction

The way towards recognition of the role of unknown cosmophysical effects on the Earth processes presents certain difficulties. At the first stage of research, the existence of non-electromagnetic radiation affecting the physical and biological systems was hypothesized. Among these, the conclusion about the advanced (4–6 days lead time) increase of corynebacteria sensitivity to the emergence of active formations on the surface of the Sun made by A. L. Chizhevsky and S. T. Velkhover [1] should be mentioned. It may be only assumed that these formations are linked to perturbations in the deep spheres of the Sun and are accompanied by the topography changes in its gravitational field. At least, this is supported by the existence of lead time phenomenon undetected by other methods.

The applied research of the cosmophysical radiation and its impact on physical systems started with the works of N. A. Kozyrev [2], who had registered with a telescopic system the effect of unknown factor of high penetrating power. Due to the fact that the optical entrance of the telescope was overlaid with a metal screen, a non-electromagnetic origin of the registered radiation may be suggested. The results received by N. A. Kozyrev were confirmed later, in the experiments of the workgroup headed by M. M. Lavrentiev, Fellow Russian Academy [3]. Valuable results were obtained at the recent stage of research [4–8].

2 Studies of pulsed signals in photocurrent measurements with PCC-2

Technical characteristics of PCC-2 instrument: Photoelectric concentration colorimeter (PCC-2) is designed for measuring coefficients of transmission and optical density of solutions in the range of 315–980 nm (a set of optical light filters), as well as to determine the concentration of substances in solution by constructing calibration curves. Radiation detectors: F-26 photocell for operating in 315–540 nm range and FD-7K photodiode for operating in 590–980 nm range (Fig. 1).

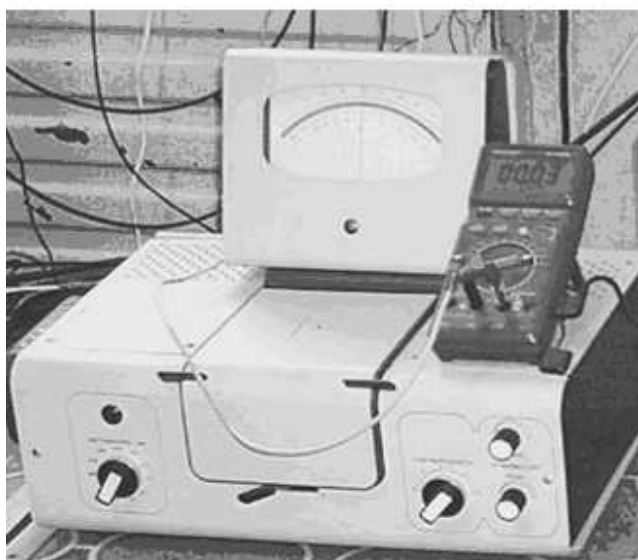


Fig. 1: Photoelectric concentration colorimeter (PCC-2).

Recording device of the instrument is M 907-10 microammeter with digitized scale for coefficients of transmission and optical density. Power supply 220 ± 22 V, $50/60 \pm 0.5$ Hz. The source of radiation – KGM 6.3–15 small-size halogen lamp. The range of readings that characterizes random errors does not exceed 0.3%.

The normal running conditions for PCC-2 are: temperature $(20 \pm 5)^\circ\text{C}$, relative humidity 45–80%, mains voltage 220 ± 4.4 V, 50 Hz.

In the course of the Antarctic expedition to Mirny station, 1996–1997, during measurements of the dynamics rate of biochemical reactions [9], sharp microammeter deflections on PCC-2 panel were recorded, which corresponded to the increased optical density of the reaction under study. Since the bursts are uncharacteristic of the instrument properties and admissible estimates under the experimental procedure, it was

suggested that the reason for the observed bursts might be associated with non-trivial fluctuations (pulsed signals) [10, 11]. The general characteristics of pulsed signals is as follows:

- The polarity of pulsed signals corresponded to the decrease of photocurrent magnitude;
- Pulsed signals were observed at any time of the day, including around midnight;
- The duration of bursts was less than one second;
- Bursts were registered under various shielded conditions in the laboratory building coated with duralumin sheets (Antarctica); in ship-board space, multiple-shielded by steel deck grillage (RSV “Akademik Fedorov”); and in a cast-concrete building (AARI, St.Petersburg). The intensity of pulsed signals in Antarctica was considerably higher than in St.Petersburg;
- Pulsed signals have no geographic restrictions, they were recorded both in the Southern and Northern hemispheres, from 70°S (Antarctica, 2000) to 86°N (Arctic, 2000).

Since the receiving unit in the instrument is represented by a photocell, where the photocurrent is recorded with a micro-ammeter, variation recording on the instrument panel was transformed through the recording of photocurrent values in the absence of working substance. Testing of photocurrent measurements was performed in a cast-concrete building (AARI, St. Petersburg) in automatic mode via the COM-port of a PC, using DM3600 digital multimeter. The experiment was supplemented by PCC-2 thermal stabilization 20°C (± 1). Uninterrupted power supply to the entire system was ensured by UPS-525 bt. In the course of measurements, abrupt changes of photocurrent in the form of a pulsed signal, in the direction of its decrease, was recorded. Sample registration of pulsed signals in photocurrent is shown in Fig. 2.

The practice of geophysical observation involves methods of testing the effects of artificial electromagnetic interference on the recording systems. Testing may be valid if the experiment is placed away from the metropolis, to minimize the impact of anthropogenic factors. Following these requirements, photocurrent measurements with PCC-2 were conducted at Novolazarevskaya station (Antarctica) in 2004.

3 Checking the integrity of the experiment

At the primary stage of automated measurements, PCC-2 sensitivity to the effects of artificial electromagnetic field (AEMF) was tested. The following instruments were used in the experiment:

1. Coil—to generate an electromagnetic field:
 - Radius of turn: 0.055 m;

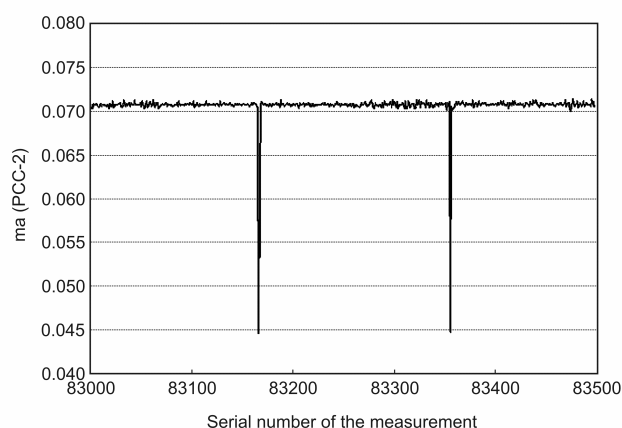


Fig. 2: Sample registration of pulsed signals in photocurrent (PCC-2)

- Coil dimensions: width of turn—0.07 m, diameter—0.11 m;
 - Number of turns: 17;
2. Self-contained DC power source: storage battery 24 V, 75 A×hour;
 3. Dropping resistor $R_D = 2$ Ohms;
 4. “Mastech” M-832 digital multimeter;
 5. Stationary recording magnetometer at Novolazarevskaya station;
 6. PCC-2 photocurrent recording system:
 - PCC-2 microphotocolorimeter;
 - M3850D digital multimeter (with RS-232 cable outlet);
 - Power supply unit for multimeter.

The magnetic field was excited by a pulsed current without a dropping resistor. The protocol of PCC-2 testing effects is provided in Table 1.

3.1 Measurements of the magnetic field generated by the coil

Measurements of the magnetic field induced by coil were conducted with stationary recording magnetometer (SRM) at Novolazarevskaya station. The magnetic field was excited by a pulsed current without a dropping resistor, and by a constant current with a dropping resistor ($R = 2$ Ohms). Generation of DC magnetic field for longer than 1 second without limiting resistance was not possible, because the strength of current could be as high as 100A against the resistance of coil ~ 0.2 Ohms. For this case, the magnetic field of coil was measured additionally with dropping resistor included in the circuit.

3.2 Measurement results

Since the three-component magnetic variometer can not be considered as a point-source instrument at a distance of 1 me-

| Time (GMT) | The distance to the PCC-2 | The position of the coil | The mode of influence | Vector magnitude of induction of a magnetic field (nT) |
|------------|---------------------------|--------------------------|---|--|
| 16:16:30 | 1.5 m | vertical | a single pulse pulse duration ~ 0.2 c | 450 – 900 |
| 16:17:00 | 1.5 m | vertical | a single pulse pulse duration ~ 0.2 c | 450 – 900 |
| 16:17:35 | 1.5 m | vertical | a single pulse pulse duration ~ 0.2 c | 450 – 900 |
| 16:18:20 | 1.5 m | horizontal E-W | a single pulse pulse duration ~ 0.2 c | 450 – 900 |
| 16:18:30 | 1.5 m | horizontal E-W | a single pulse pulse duration ~ 0.2 c | 450 – 900 |
| 16:18:40 | 1.5 m | horizontal E-W | a single pulse pulse duration ~ 0.2 c | 450 – 900 |
| 16:19:30 | 1.5 m | horizontal N-S | a single pulse pulse duration ~ 0.2 c | 450 – 900 |
| 16:19:45 | 1.5 m | horizontal N-S | a single pulse pulse duration ~ 0.2 c | 450 – 900 |
| 16:20:00 | 1.5 m | horizontal N-S | a single pulse pulse duration ~ 0.2 c | 450 – 900 |
| 16:20:15 | 1.5 m | horizontal N-S | a single pulse pulse duration ~ 0.2 c | 450 – 900 |
| 16:21:30 | 1.9 m | vertical | a single pulse pulse duration ~ 0.2 c | 250 – 500 |
| 16:21:40 | 1.9 m | vertical | a single pulse pulse duration ~ 0.2 c | 250 – 500 |
| 16:21:45 | 1.9 m | vertical | a single pulse pulse duration ~ 0.2 c | 250 – 500 |
| 16:22:00 | 1.9 m | horizontal E-W | a single pulse pulse duration ~ 0.2 c | 250 – 500 |
| 16:22:10 | 1.9 m | horizontal E-W | a single pulse pulse duration ~ 0.2 c | 250 – 500 |
| 16:22:15 | 1.9 m | horizontal E-W | a single pulse pulse duration ~ 0.2 c | 250 – 500 |
| 16:23:00 | 1.9 m | horizontal N-S | a single pulse pulse duration ~ 0.2 c | 250 – 500 |
| 16:23:10 | 1.9 m | horizontal N-S | a single pulse pulse duration ~ 0.2 c | 250 – 500 |
| 16:23:15 | 1.9 m | horizontal N-S | a single pulse pulse duration ~ 0.2 c | 250 – 500 |

Table 1: Results of AEMF testing effects on PCC-2.

ter (three sensors located along a straight line, at a distance of 16 cm), the numeric value (module of vector) of magnetic induction in the coil with current could be calculated only approximately, based on the data from three variometers. Variations in 3 components of the magnetic field were registered – D (WE), H (SN), and Z (vertical). Module of the vector T was calculated by the equation:

$$T = \sqrt{\Delta D^2 + \Delta H^2 + \Delta Z^2}. \quad (1)$$

The results of calculations are presented in Table 2.

Given that the value of coil resistance R_{cat} equaled 0.2 Ohms and in dropping resistor 2 Ohms, it could be expected that the magnetic field in the coil carrying current would be ~ 10 times higher with the switched dropping resistance than without it. However, we did not account for the internal resistance of the battery, which depends both on the current frequency (essential in case of a current pulse) and its strength. Table 2 demonstrates that other conditions being equal, a coil powered by the same battery creates a magnetic field, which is 4–5 times greater under dropping resistor, as compared to the field generated without it. This ratio is probably even more, due to the low frequency of ADC sampling used in measurements of pulsed fields.

As is known, the maximum and minimum values of magnetic induction vector differ two-fold exactly, if measured equidistant from the center of the magnetic dipole. The coil size being ~ 0.1 m, the field of the coil can be regarded with good accuracy as a dipole field, at a distance above 1 m from its center. Thus, when the coil is powered by a battery in a pulsed mode, magnetic induction measured at 1 m off the coil center ranges from 1500 nT (in the plane perpendicular to the coil axis) to 3000 nT (on its axis). The findings of the experiment showed that the photocurrent readings in PCC-2 are not affected by pulsed electromagnetic field with the magnetic component value > 6000 nT, which is greater by 2–3 orders of magnitude than the maximum amplitude of geomagnetic pulsations at 0.1–0.001 Hz frequencies, and several times higher than the intensity of the strongest magnetic storms. The second experiment on the effects on PCC-2 was conducted with high-frequency transmitter (1782 MHz), ACS-1 radiosonde aerological service at Novolazarevskaya station. Characteristics of the transmitter: — Operating frequency 1782 ± 20 MHz — Pulse recurrence frequency 457.5 ± 0.2 Hz — Pulse duration 1 mcs — Transmitter power 2 W / 300 W The distance between the PCC-2 location “geophysicists’ premises”) and the aerological service was measured with a GPS receiver and made 145 ± 15 m along a straight line. Effects of ACS-1 were estimated through sessions, of 18 minutes total duration, in 2 W and 300 W modes.

Emission series under transmitter power 2W: a) from 22^h 34^m till 22^h at 37 m, at 0° vertical deviation b) from 22^h 37^m till 22^h 39^m, at +1° vertical deviation c) from 22^h 39^m till 22^h 43^m, at +3° vertical deviation, aimed to receive the signal reflected from the adjacent rocks (~ 50 m) and the ice cap

(~ 500 m). The signal reflected from the ice cap was fixed on the radar screen. The signal reflected from the rocks was within the measurement error, due to time delay arising from the proximity to the transmitter. Emission series under transmitter power 300W: a) from 22^h 51^m till 22^h 56^m, at 0° vertical deviation b) from 22^h 56^m till 22^h 59^m, at +1° vertical deviation c) from 22^h 59^m till 23^h 02^m, at 1° vertical deviation.

The experimental result proved that photocurrent readings are unaffected by PCC-2 exposure to the high-frequency electromagnetic field.

4 Data analysis and search of driving factor

Data processing and analysis of photocurrent measurements were carried out with “Statistica” software using the following statistical methods:

- Calculation of the parameters of the distribution (standard error, standard deviation, variance);

$$S = \sqrt{\frac{1}{n-1} \sum_{i=1}^n (x_i - \bar{x})^2}. \quad (2)$$

- Spectral (Fourier) analysis (periodograms, estimate of the spectral density), cross-analysis, the value of coherence;
- Identification of the time series model (trend analysis), and analysis of the inadequacy of the model (analysis of residuals), $e_i = (y_i - y_i - hat)$;
- Parabolic polynomial interpolation of the best approximation $y = b_0 + b_1x + b_2x^2 + b_3x^3 + \dots + b_nx^n$;
- Selection of the filtering method, use of the moving average (from 3 to 23 points);
- Cross-correlation, correlation factor (r).

During the period of photocurrent measurements with PCC-2 at Novolazarevskaya station, from 24.04.2004 till 01.02.2006, over 20,000 events of pulsed signals were registered. The average daily number of signals comprised ~ 300 events, with a minimum of about 80 and a maximum of 580 events. All registered signals are characterized by the polarity in the direction of decreasing photocurrent, 30–50%, on average. The long-period variations of about one year duration may be distinguished in the general distribution pattern of pulsed signals (Fig. 3). The figure also reveals that broad maxima correspond to the end periods of the polar night (July–August). Hence, the number of signals (intensity) does not depend on the influx of solar radiation. In search for the connection of these variations with cosmophysical factors, attention was given to the annual Earth motion along the orbit (the ecliptic). As is known, the equation of time [12] is the sum of two following components. These are the *eccentricity equation* and the *ecliptic inclination equation* (the declination

| Time (GMT) | The distance to the SRM | The position of the coil | The mode of influence | Vector magnitude of induction of a magnetic field (nT) |
|---------------------------------|-------------------------|--------------------------|---|--|
| 15.07.2006 14:03:10–14:03:16 | 2 m | horizontal E-W | a single pulse pulse duration ~ 0.2 c | ~ 200 nT |
| 15.07.2006 14:06:33–14:06:34 | 1.5 m | horizontal E-W | a single pulse pulse duration ~ 0.2 c | ~ 700 nT |
| 15.07.2006 14:09:42–14:09:51 | 1 m | vertical | a single pulse pulse duration ~ 0.2 c | ~ 2500 nT |
| 20.07.2006 10:43:30–10:44:00 | 1 m | vertical | constant field | ~ 600 nT |
| 20.07.2006 10:51:00–10:51:35 | 1 m | vertical | constant field | ~ 650 nT |
| 20.07.2006 10:53:45–10:54:15 | 1 m | vertical | constant field | ~ 550 nT |
| 20.07.2006 10:56:45–10:57:15 | 1 m | horizontal E-W | constant field | ~ 360 nT |

Table 2: Results of AEMF testing effects on SRM.

of the Sun). While the bonding of the connection of the signals and the *ecliptic inclination equation*, we obtained a correlation whose coefficient is close to $r \sim 0.7$. Fig. 3 (a, b) gives the comparison of the numerical values of the daily impulse signals in the photocurrent (KFK-2) and the numerical values of the Sun's declination during 24.04.2004–01.02.2006.

In general distribution of the signals, variations of different duration are traced. Their behavior was identified by comparing the total signal distribution with the indices of solar activity and the total solar radiation (TSI), as well as with fluxes of solar cosmic rays and geomagnetic activity indices. These comparisons revealed that the changes of the daily values of signals best correspond to the SA F10.7 cm index changes and the average daily standard deviation of energy TSI (SD). Standard deviation (SD) shows the variance of the random variable values, with respect to its statistical expectation, i.e., the rate of within-group variability of a given indicator. Comparisons of the series are shown in Figs. 4–5 (a, b). The less pronounced relationship is viewed in case of K-index (Fig. 6) and the SCR fluxes (Fig. 7). Figure 7 demonstrates good matching in the value's trends starting from 425 days (late June 2005).

5 The parallel measurements of the photocurrent (KFK-2) and the fluctuations at the 520 nm wavelength, in the light-emitting diode 565 nm (AvaSpec-2048).

Assuming that the effects in PCC-2 photocurrent were caused by heliophysical impact, similar effects should be expected in the readings of other instruments.

AvaSpec-2048 (www.avantes.com) is a multifunctional fiber optic spectrometer intended for a wide range of studies (Fig. 8). The spectrometer is designed on AvaBench-75 platform with symmetric optical bench (Czerny-Turner). The elemental profile of spectral distribution is read by the operated

electronic board and is further transferred from the detector matrix to PC via USB/RS-232.

The task of the second experiment was to conduct “PCC-2–AvaSpec–2048” parallel measurements referenced to GPS universal time. The measurements were performed from 16.05.05 till 01.11.05, with spatial separation of the instruments up to 5 m distance, in a continuous automatic mode. When processing fluctuations in different LED (565nm) spectral lines, the 520 nm line was selected, where the observed pulsed signals had the same specifics as in PCC-2. Fig. 9 shows an example of the registration. The first estimates of fluctuations comparing the two methods were obtained for the period from 31.05.04 till 08.09.04. Figure 10 shows the temporal comparisons for daily values of bursts in photocurrent FD-7K and energy fluctuations the wavelength 520 nm converted into the average daily standard deviation (SD).

6 Parallel measurements of photocurrent (PCC-2) and fluctuations within the 339.5–346 nm range of the atmosphere zenith (AvaSpec–2048)

Measurements of fluctuations within the 339.5–346 nm range of the atmosphere zenith were conducted with fiber optic spectrometer AvaSpec–2048. The data acquisition chart on spectral zenith observations of solar UV–radiation is presented in Fig. 11.

The measurements were performed during the polar summer, in accordance with the methodology of zenith observations on the ozone content, at the Sun angle $> 5^\circ$. Data were recorded in the files in automatic mode, with a sampling interval of 2–3 seconds. Observations were accompanied by time corrections from GPS. The initial phase of observations aimed at the search of non-instrumental fluctuations at the full range of frequencies, within 297–780 nm range. At 0.3 nm resolution of diffraction grating, more than 1,300 spectrum lines were analyzed. To conduct parallel measurements with

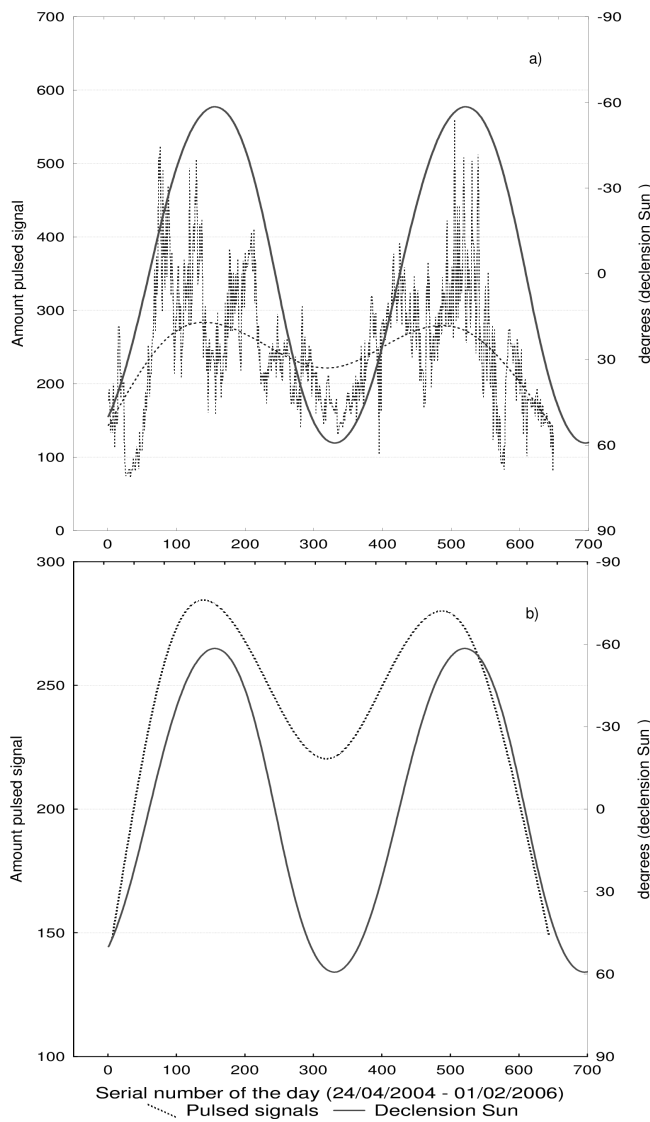


Fig. 3: the comparison of the distributions of the daily numerical values of the impulse signals of KFK-2 and the general number polynomial b) and the ecliptic inclination (the declination of the Sun) during 24.04.2004–01.02.2006 (Novolazarevskaya station).

the spectrometer and PCC-2, four ranges of the atmosphere zenith spectrum were selected (303–305 nm, 331–332.5 nm, 329.5–334 nm, 339.5–346 nm), for which the standard deviation of energy (SD_E) exceeded the instrumental fluctuations by an order, or above [13, 14]. Figure 12 shows a sample recording of fluctuations in the range of 339.5–346 nm. The profile demonstrates bipolar fluctuations reaching 339.5 nm and 346 nm levels, measured in the center of 342.5-nm frequency range.

The energy estimates (eV/photon) of pulsed signals were defined. For example, according to the formula:

$$\text{photon energy } E(\lambda) = \frac{hc}{\lambda_e}, \quad (3)$$

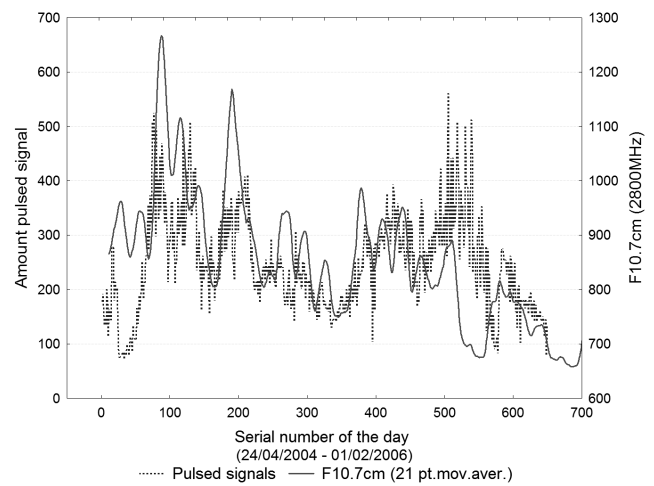


Fig. 4: Comparison of temporal changes in solar activity index F10.7 cm (2800 MHz) with distribution of the daily values of pulsed signals in PCC-2, for the period 24.04.2004–01.02.2006 (Novolazarevskaya station).

where, h = Planck's constant $6.62606876 \times 10^{-34}$, c = velocity of light, 2.998×10^8 m/s; λ = wavelength in meters.

The average estimates of pulsed signals of energy within the 339.5–346 nm range were as follows:

$$E_{min} (346\text{nm}) = 3.583 \text{ (eV/photons)},$$

$$E_{mean} (342.5\text{nm}) = 3.619 \text{ (eV/photons)},$$

$$E_{max} (339.5\text{nm}) = 3.652 \text{ (eV/photons)}.$$

Comparison of fluctuations within the tested ranges with pulsed signals in PCC-2 showed an ambiguous correlation. The most consistent changes in PCC-2 pulsed signals were observed within a 339.5–346 nm range. Comparison of the series for the period from 25.09.07 till 17.12.07 illustrates this example in Fig. 13.

7 Prognostic functionalities of the observed effects

In addition to the obtained results, the general distribution pattern was detected in the daily values of pulsed signals measured with PCC-2, which corresponded to ≈ 300 -day cycle. This period was revealed through the comparison of the annual intervals of the general series, with a difference of about two months. The second interval was compared to the first against the difference minus ≈ 60 days from the start of the first interval. For example, the top graph in Figure 14 (a, b) shows the intervals comparison for 24.04.2004–23.04.2005 and 21.02.2005–01.02.2006. On the bottom figure, the cross-correlation function of two series by logs, with corresponding correlation factors, is shown. It can be seen that the maximum correlation value reaches $r \sim 0.7$. Assuming all the above relationships between pulsed signals and variations of the SA index and TSI, a 300-day cycle was also detected in the F10.7 cm index and TSI. A comparison of F10.7 cm and TSI distribution patterns within the annual intervals is provided in

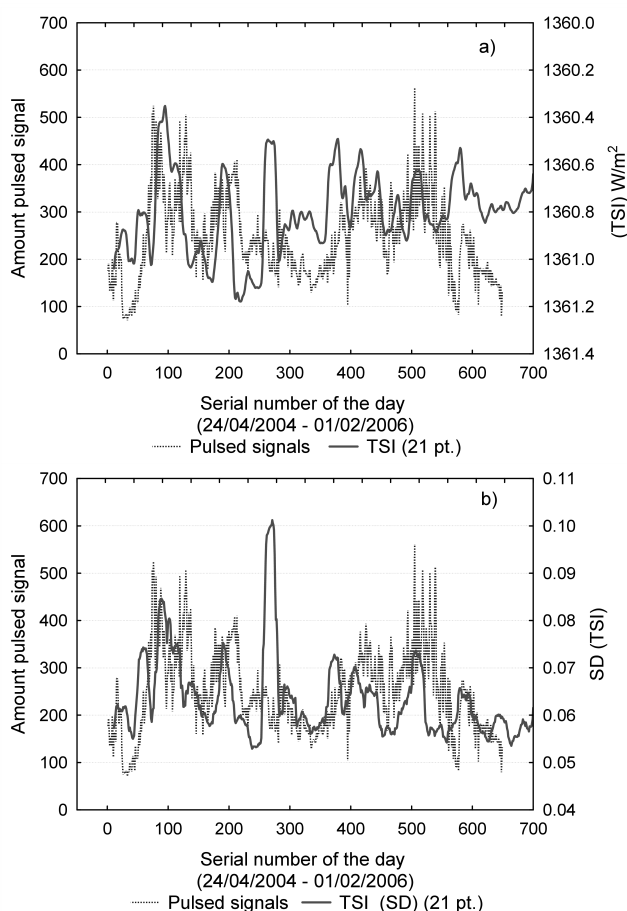


Fig. 5: Comparison of temporal changes in energy TSI, and b) — Comparison of the daily average standard deviation TSI (SD) with distribution of the daily values of pulsed signals in PCC-2, for the period from 24.04.2004 till 01.02.2006 (Novolazarevskaya station).

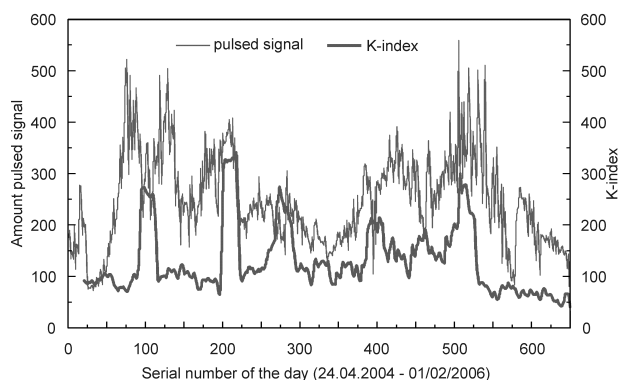


Fig. 6: Comparison of temporal changes in K-index variations with distribution of the daily values of pulsed signals in PCC-2, for the period from 24.04.2004 till 01.02.2006 (Novolazarevskaya station).

Fig. 15 (a, b): 24.04.2004–24.04.2005 and 24.02.2005–01.02.2006. Figure 15 (a) indicates the matching of F10.7 cm index variation in phase opposition of variations.

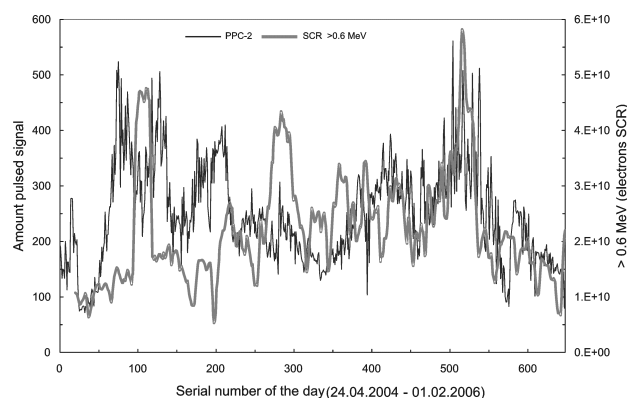


Fig. 7: Comparison of the temporal changes in SCR electron variations (> 0.6 MeV) with distribution of the daily values of pulsed signals in PCC-2, for the period from 24.04.2004 till 01.02.2006 (Novolazarevskaya station).

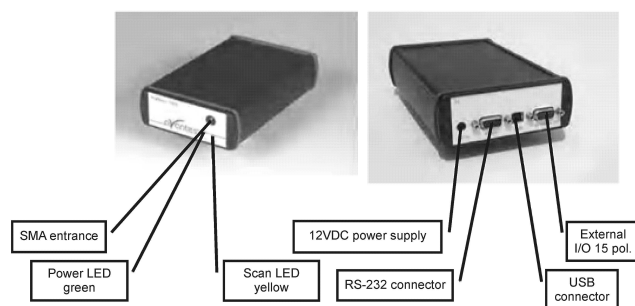


Fig. 8: Spectrometer AvaSpec-2048 (www.avantes.com).

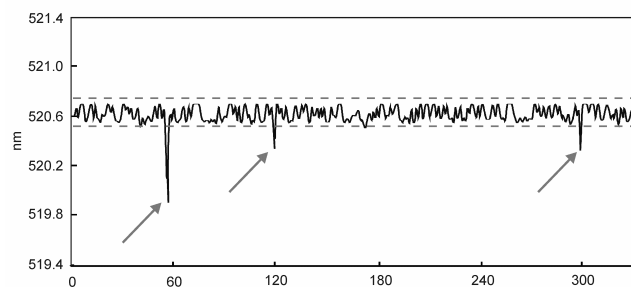


Fig. 9: Sample recording of pulsed signals at 520-nm frequency in 565-nm LED spectrum (AvaSpec-2048) (Novolazarevskaya station).

Comparison is presented upon the unfiltered values (without leveling). Unlike F10.7 cm, the daily average standard deviation of the energy TSI reveal matching of variations in the same phase character but if applying the moving average filter to 21 pts. The maximum amplitude in SD (TSI) is associated with a solar flare.

As regards the contribution of geomagnetic factors to the 300-day period, its manifestation was traced in the interplanetary magnetic field component (By). Figure 16 shows the comparison of By values for the intervals 01.01.2003–

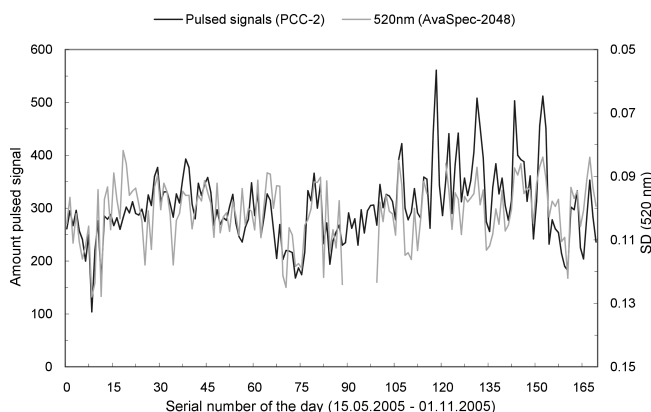


Fig. 10: Comparison of daily values of bursts in photocurrent with the average daily standard deviation (SD) of fluctuations at the 520 nm wavelength (AvaSpec-2048), for the period from 15.05.05 to 01.11.05 (Novolazarevskaya station).

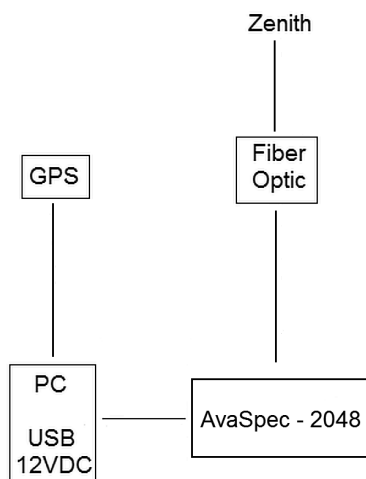


Fig. 11: Data acquisition chart on spectral zenith observations of solar UV-radiation in the atmosphere zenith (Novolazarevskaya station).

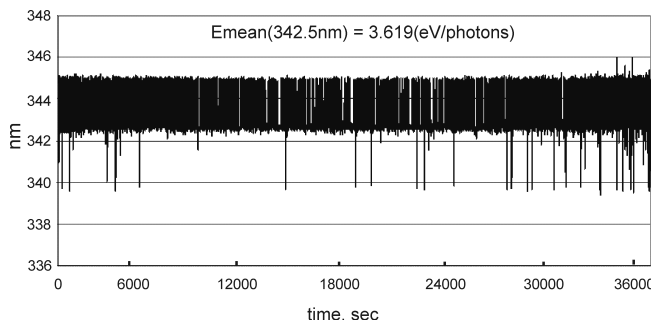


Fig. 12: Sample registration of fluctuations in 339.5–346 nm range (AvaSpec-2048), at clear atmosphere zenith, from 07h 00m till 17h 00m (09.03.2005, Novolazarevskaya station).

01.01.2004 and 27.10.2003–27.10.2004. The identity in variations and the phase convergence of the series, as demon-

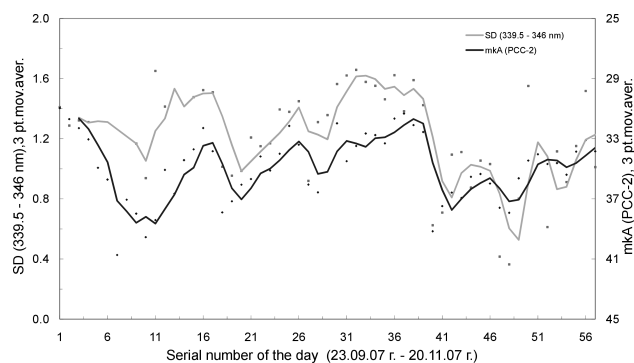


Fig. 13: Comparison of the daily average standard deviation of fluctuations in energy (SD_E) within the 339.5–346 nm range (AvaSpec-2048) in the atmosphere zenith and PCC-2 pulsed signals, for the period from 23.09.07 to 20.11.07 (Novolazarevskaya station).

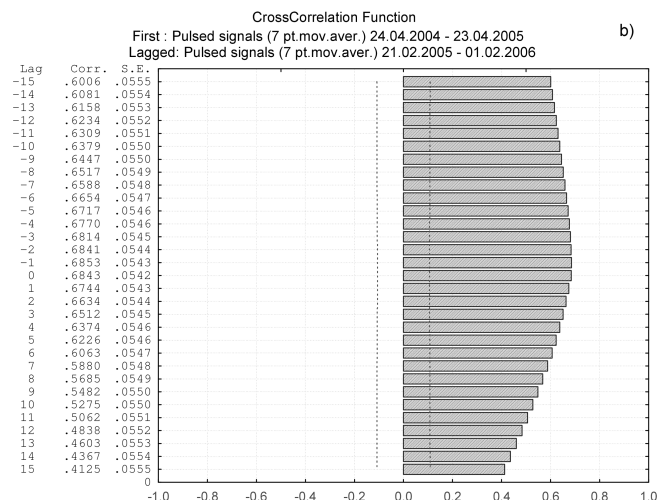
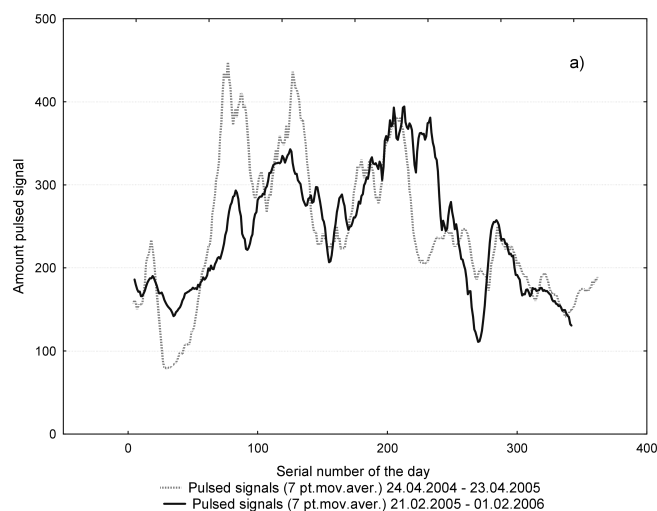


Fig. 14: Comparison of PCC-2 daily values of pulsed signals within the intervals 24.04.2004–24.04.2005 (a) and 21.02.2005–01.02.2006 (b) (Novolazarevskaya station).

strated in Figure 16, is the most indicative of the existence of the 300-day cycle. As in the case with F10.7 cm, unfil-

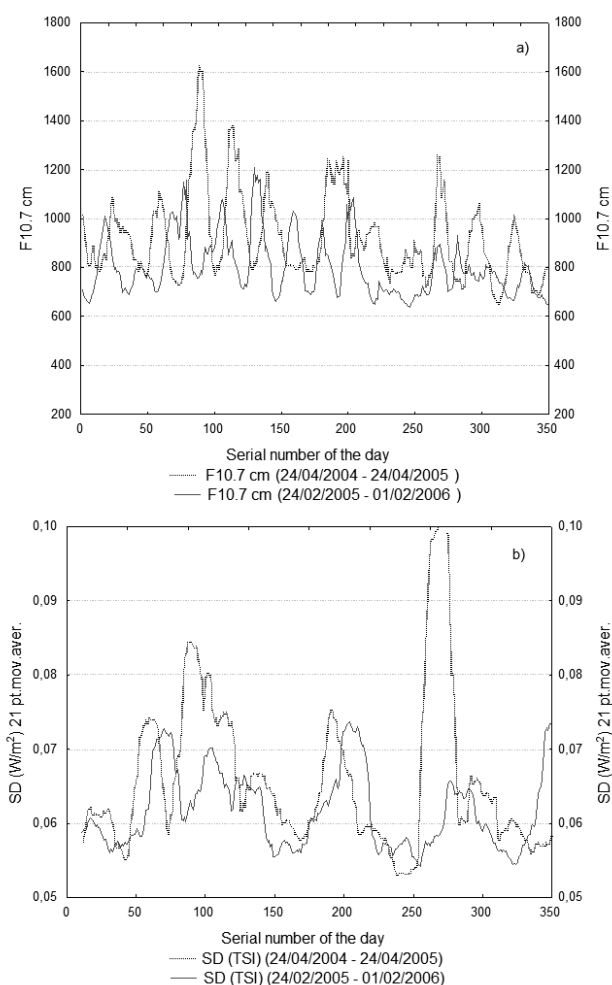


Fig. 15: Comparison of F10.7 cm and TSI distribution patterns within the intervals 24.04.2004–24.04.2005 (a) and 24.02.2005–01.02.2006 (b).

tered series were compared. This convincing fact is not yet explained through the known mechanisms of solar-terrestrial relationships.

Thus, pulsed signals bear prognostic characteristics associated, in our opinion, with the unknown heliophysical factor.

Similar results were obtained under extensive laboratory experiments conducted by Sergey Korotaev at Geoelectromagnetic Research Institute RAS (Troitsk, Moscow Region, Russia) [6].

His publication considers the phenomenon of non-locality and correlation of isolated dissipative processes, as well as description of the experiment and the results of investigations. Using two types of detectors based on the link between the entropy and the potential barrier height U , reliable correlations were established between: lead variations of dark current and temporal events in the atmospheric pressure (69, 73 days), variations of geomagnetic activity (Dst-index) (33 days) and variations of the F10.7 cm index (42 days). Based

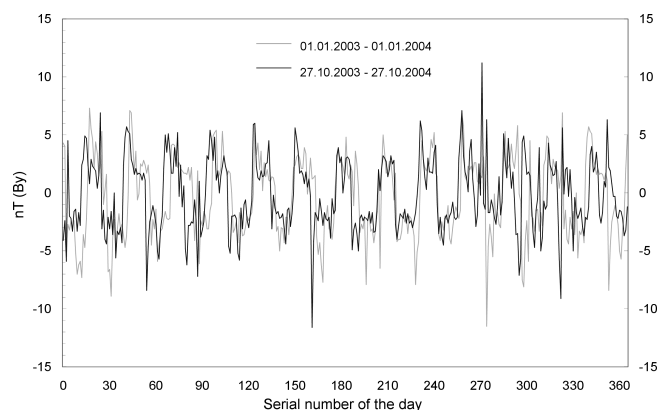


Fig. 16: Comparison of variations of the interplanetary magnetic field component B_y , by intervals: 01.01.2003–01.01.2004 and 27.10.2003–27.10.2004.

on the established correlations between the detectors and SA, the author established a temporal range of the lead coupling, from 42 to 280 days.

8 Conclusion

In our assumptions on the source of pulsed signals, the impact of cosmic particles fluxes and their secondary radiation (protons and products of their interaction with atmospheric nuclei — *positrons, muons, pi-mesons, K-mesons, electron pairs, gamma ray quanta, atmospheric neutrinos*, etc.) should be first considered. In determining the relation of the observed pulsed effects to the secondary cosmic rays, a comparison of distribution of pulse signals with variations of atmospheric cosmic rays of geomagnetic, solar and galactic origin would be quite sufficient. Assuming that similar pattern in temporal variations of the compared series would persist for a long time interval (within months), the penetrating component should be identified, since pulses are observed in shielded conditions. The penetrating component of cosmic rays can be defined by the type of interaction of cosmic rays with the substance.

For instance, among those well-known are: the nuclear-active component, soft component of secondary cosmic rays, electron-photon showers and the penetrating component of the secondary radiation — muons and neutrinos. Of the above mentioned, muons are the most likely source, as the muon flux represents a penetrating component and, against a relatively moderate energy power (~ 10 GeV), can easily enter the atmosphere and penetrate the shielding conditions of PCC-2. However, this version contradicts with the significant differences between the diurnal statistics of muons and neutrinos and pulsed signals. E.g., according to the observations in NT-200 neutrino telescope located at a depth of 1100–1200 m in the Baikal Lake, the daily number of atmospheric muons reaches $\approx 1,000,000$ and for atmospheric neutrinos — one oc-

currence in two days, on average.*

The hypothetical factor of heliophysical origin that causes simultaneous effects in photocurrent, the LED spectrum, and the zenith spectrum of the atmosphere, remains unknown. On the one hand, a good coincidence between the number of signals and variations in F10.7cm and TSI is observed, which may be regarded as conclusive indication of their solar origin. On the other hand, signals are registered, regardless of the shielding conditions, which is indicative of a high penetration capacity of the heliophysical factor. Further, no reliable evidence of a link between pulsed signals, cosmic ray fluxes and geomagnetic activity is revealed. It is as well obvious that the known mechanisms of the solar-terrestrial relationships do not represent direct implications of the effects observed in the experiment. An especially characteristic indicator of the signal intensity is the statistical correlation with the declination of the Sun, i.e., the position of the Earth on the orbit (the ecliptic). We do not exclude the assumption about the directed impact of this "hypothetical" factor in the ecliptic plane.

According to the results demonstrated in figures 14–16, it is evident that the studied pulsed signals in photocurrent have 60–65 days lead time, on average, compared to the solar events. If such pattern is scaled against the 11-year cycle of the solar activity (SA), we should expect that solar variations, recurrent in 300 days, would return to the starting point in 5.5 years (in our case, the measurement starting point was 24.04.2004), which makes approximately a half of the 11-year SA cycle. This presents a point of interest. The solar cycles are known to have a progression: 11-year, 22-year, 44-year, 88-year, etc. According to our results, we can not exclude the possibility of declining values of the SA cycles, down to 5.5 years, or less. Possibly, the 300-day cycle refers to the initial cycles in this progression. Its physical component may be determined by the processes occurring in the central zone of the Sun.

Submitted on: April 26, 2013 / Accepted on: May 06, 2013

References

1. Chizhevsky A.L. Cosmic pulse of life. Mysl', Moscow, 1995.
2. Kozyrev N.A. Selected Papers. Leningrad Univ. Publ., Leningrad, 1991.
3. Lavrent'ev M.M., and others. On the registration of the true position of the Sun. *Doklady AN USSR*, 1990, v.315, no.2, 368–370.
4. Shnol' S.E., and others. Regular variation of the fine structure of statistical distributions as a consequence of cosmophysical agents. *Physics-Uspekhi*, 2000, v.170, no.2, 214–218.
5. Parkhomov A.G., Maklyaev E.F. Research on rhythms and fluctuations through long-term measurement of radioactivity, crystal frequency, semiconductor noise, temperature and atmosphere pressure. *Fizicheskaya Mysl' Rossii (Russian Physics Reports)*, 2005, no.1, 1–12.
6. Korotayev S.M. Heliogeophysical nonlocality effects — shadows of future in the present. *Quantum Magic*, 2004, v.1, issue 2, 2219–2240.
7. Kondratyev K.Y., Nikol'skiy G.A. Impact of solar activity on structure components of the Earth. *Issledovanie Zemli iz Kosmosa*, 2005, no.3, 1–10.
8. Sizov A.D. Current fluctuations in the Wheatstone bridge. Possible cosmophysical correlations. *Biofizika (Biophysics)*, 1998, v.43, issue 4, 726–729.
9. Gorshkov E.S., Shapovalov S.N., Sokolovskiy V.V., Troshichev O.A. On the reaction rate of the unitiol oxidation by nitrite ion. *Biofizika (Biophysics)*, 2000, v.45, issue 4, 631–635.
10. Shapovalov S.N., Gorshkov E.S., Troshichev O.A. Cosmophysical effects observed in impulses of the microphotocolorimeter current. *Biofizika (Biophysics)*, 2004, v.49, Suppl. 1, 119–121.
11. Shapovalov S.N., Troshichev O.A., Povazhny V.I. Study of short time pulses in the photoelectric effect under conditions of Antarctica (station Novolazarevskaya). *T2-8 Heliosphere Impact on Geospace IPY Oslo Science Conference*, 08–12 June 2010.
12. The Astronomical Calendar (permanent part). Nauka, Moscow, 1981.
13. Troshichev O.A., Shapovalov S.N., Lozovsky V.T. Study of pulsed signals in UV spectra lines of free atmosphere above Novolazarevskaya station (Antarctica): effect of the solar irradiance? *37th COSPAR Scientific Assembly*, 13–20 July 2008, Montreal, Canada, p.322.
14. Shapovalov S.N., Troshichev O.A. Study of pulsed energy fluctuations and solar UV variations by data of spectral measurements in zenith of free atmosphere at Novolazarevskaya station (Antarctica). *39th COSPAR Scientific Assembly*, 14–22 July 2012, Mysore, India (C2.3-0009-12).

*http://nuclphys.sinp.msu.ru/neutrino/newtrino_s/baik.htm